



## Fuzzy topology-based method for unsupervised change detection

Wenzhong Shi, Pan Shao, Ming Hao, Pengfei He & Jianming Wang

To cite this article: Wenzhong Shi, Pan Shao, Ming Hao, Pengfei He & Jianming Wang (2016) Fuzzy topology-based method for unsupervised change detection, Remote Sensing Letters, 7:1, 81-90, DOI: [10.1080/2150704X.2015.1109155](https://doi.org/10.1080/2150704X.2015.1109155)

To link to this article: <http://dx.doi.org/10.1080/2150704X.2015.1109155>



Published online: 03 Nov 2015.



Submit your article to this journal [↗](#)



Article views: 50



View related articles [↗](#)



View Crossmark data [↗](#)



## Fuzzy topology–based method for unsupervised change detection

Wenzhong Shi<sup>a</sup>, Pan Shao<sup>b</sup>, Ming Hao<sup>c</sup>, Pengfei He<sup>c</sup> and Jianming Wang<sup>b</sup>

<sup>a</sup>Joint Research Laboratory on Spatial Information, The Hong Kong Polytechnic University and Wuhan University, Hong Kong and Wuhan, China; <sup>b</sup>School of Remote Sensing and Information Engineering, Wuhan University, Wuhan, China; <sup>c</sup>Jiangsu Key Laboratory of Resources and Environmental Information Engineering, China University of Mining and Technology, Xuzhou, China

### ABSTRACT

This letter presents a novel framework for the analysis of difference image (DI) in unsupervised change detection problems based on fuzzy topology. First, the DI is softly categorized into unchanged and changed classes. In other words, a membership function is computed for each class. Second, each class is decomposed into three parts – interior, fuzzy boundary and exterior – by analysing its membership function through fuzzy topology. Third, for each class, its interior pixels which have a high membership degree are classified as the current class; its exterior, denoting the interior and fuzzy boundary parts of the other class, is ignored; and its fuzzy boundary pixels associated with a low membership degree are reclassified using the supported connectivity in fuzzy topology. As a result, the proposed approach can solve the problem of misclassifying pixels in the fuzzy boundary of unchanged or changed class to some extent, providing improved change detection accuracy. Experiments were conducted on two different datasets and the results confirm the effectiveness of the proposed framework.

### ARTICLE HISTORY

Received 12 June 2015

Accepted 1 October 2015

## 1. Introduction

In remote sensing, change detection is the process of identifying land cover changes using multitemporal remote sensing images (Bruzzone and Bovolo 2013). In the past decades, many change detection approaches have been imposed for different types of remotely sensed data. The methods can be broadly categorized into either supervised or unsupervised change detection. This paper focuses on the unsupervised change detection.

One of the most widely used types of unsupervised change detection methods is to analyse the difference image (DI). Several techniques can be applied to discriminate unchanged and changed pixels in the DI like histogram thresholding (Patra, Ghosh, and Ghosh 2011; Bruzzone and Prieto 2000), active contour model (ACM) (Bazi *et al.* 2010), dual-tree wavelet transform (Celik and Ma 2010), support vector machine (SVM) (Bovolo, Bruzzone, and Marconcini 2008), fuzzy c-means (FCM) (Ghosh, Mishra, and Ghosh 2011), etc. Thresholding is the most widely used and the simplest technique. Many known methods can be used to determine the decision threshold like Otsu algorithm (Patra,

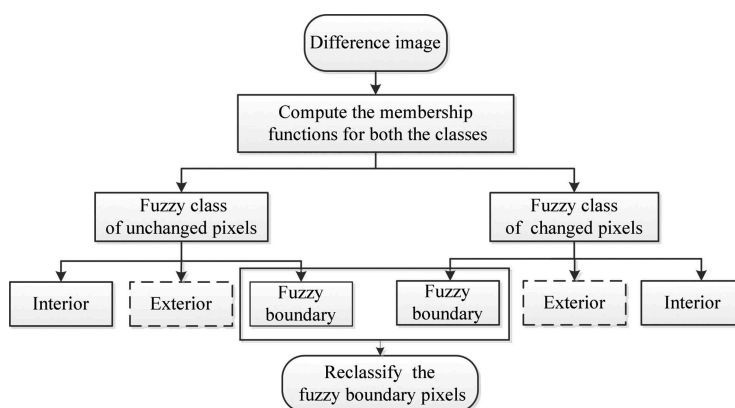


**Figure 1.** The flowchart of the proposed FTCD framework.

Ghosh, and Ghosh 2011), Kapur algorithm (Patra, Ghosh, and Ghosh 2011) and expectation maximization (EM) algorithm (Bruzzone and Prieto 2000). In the existing threshold methods, the DI is sharply divided by the selected threshold  $T$  into unchanged and changed sets. However, this process is usually inappropriate to some extent because the ranges of the pixel values of DI in the unchanged and changed classes often have overlap around the threshold  $T$  (Ghosh, Mishra, and Ghosh 2011). Many pixels in the uncertainty region around  $T$  are therefore often misclassified in the change detection map (Bovolo, Bruzzone, and Marconcini 2008). To solve this problem, a possible method is to employ the fuzzy topology theory (Chang 1968; Liu and Shi 2006). By taking advantage of it, the considered uncertain region will be effectively identified and then reclassified.

This letter proposes a novel framework of the DI analysis based on fuzzy topology to enhance the performance of change detection by further dealing with pixels in the uncertain region around  $T$  (FTCD framework). As shown in Figure 1, first, the DI is softly classified into unchanged and changed classes, by computing a membership function for each class. Then, each class is decomposed into three parts – an interior, a fuzzy boundary and an exterior – utilizing fuzzy topology. Finally, for the unchanged class, its interior pixels are classified as the unchanged class; its exterior, denoting the interior and the fuzzy boundary parts of the changed class, is ignored; and the pixels in its fuzzy boundary (corresponding to the uncertain region) are reclassified using the supported connectivity of fuzzy topology (Liu and Shi 2006), which mainly exploits spatial contextual information. The same processing procedure is also executed on the changed class.

It is worth noting that different methods of estimating membership function can be employed to the first step of the proposed FTCD framework, such as the Bayes theory, the FCM and the SVM, and each will lead to a new type of change detection approach belonging to the framework. Specially, the Bayes theory is used in this study.

## 2. Proposed change detection framework

Let  $X_1$  and  $X_2$  be two coregistered and radiometrically corrected remotely sensed images with the same size of  $M \times N$  acquired in the same ground area at different times. Then, the DI denoted by  $X_D$  is generated by applying change vector analysis (CVA) technique (Ghosh, Mishra, and Ghosh 2011) to  $X_1$  and  $X_2$ .

## 2.1. Softly classify the DI

The first step of the proposed FTCD framework aims at softly classifying the DI into two opposite fuzzy classes: unchanged ( $w_1$ ) and changed ( $w_2$ ). This is accomplished by calculating a membership function for each class. In this study, the Bayes theory, which has been proved to be effective in change detection on multispectral images (Bruzzone and Prieto 2000), is adopted to calculate the membership functions in the proposed framework. Let  $P_{w_l}$  be the membership function of the class  $w_l$  ( $l = 1, 2$ ), which behaves as a probability, that is  $P_{w_1}(X_D(i, j)) + P_{w_2}(X_D(i, j)) = 1$  for every pixel  $X_D(i, j)$  in  $X_D$ . Here  $(i, j)$  denotes the coordinate of the pixel  $X_D(i, j)$ .

To compute  $P_{w_l}$  based on the Bayes theory, the main problems to be solved are the estimations of both the probability density function  $p(X_D/w_l)$  and priori probability  $P(w_l)$  of the class  $w_l$ , where  $l = 1, 2$ . Then the membership degree (posterior probability) of  $w_l$  ( $l = 1, 2$ ) for a given pixel  $X_D(i, j)$  in  $X_D$  can be derived from

$$P_{w_l}(X_D(i, j)) = \frac{P(w_l)p(X_D(i, j)/w_l)}{P(w_1)p(X_D(i, j)/w_1) + P(w_2)p(X_D(i, j)/w_2)} \quad (1)$$

In this work, we suppose that both  $p(X_D/w_1)$  and  $p(X_D/w_2)$  can be modelled by Gaussian distributions, whose reasonableness has been explained in Bovolo, Bruzzone, and Marconcini (2008) and Bruzzone and Prieto (2000). In this context, the probability density function  $p(X_D/w_l)$  can be described by the mean  $\mu_l$  and the variance  $\sigma_l^2$  of the class  $w_l$ ,  $l = 1, 2$ . To compute the membership functions  $P_{w_1}$  and  $P_{w_2}$ , the value of a set of six parameters  $\theta = \{\mu_1, \sigma_1, P(w_1), \mu_2, \sigma_2, P(w_2)\}$  must be estimated first.

With the FTCD framework based on Bayesian membership function, the uncertain problem of threshold algorithms can be solved and the performance of thresholding techniques is then improved. To compare the improvements on different methods, this study proposes two FTCD methods, namely fuzzy topology integrated EM (FT-EM) and fuzzy topology integrated Kapur (FT-Kapur). In FT-EM, the parameter set  $\theta$  is estimated using EM as shown in Bruzzone and Prieto (2000). In FT-Kapur,  $X_D$  is classified into  $w_1$  and  $w_2$  with Kapur first, and then the value of parameter set  $\theta$  is calculated from  $w_1$  and  $w_2$ .

## 2.2. Decompose DI with fuzzy topology

### 2.2.1. Fuzzy topology theory

Fuzzy set, fuzzy topology and fuzzy topological space are the three key concepts that form the theoretical basis of the proposed framework. Fuzzy set is an extension of ordinary set. Let  $\Omega$  be a nonempty universal set, and  $I = [0, 1]$ , according to Chang (1968) and Liu and Shi (2006), a fuzzy set  $A$  (Figure 2(a)) in  $\Omega$  is a mapping  $\mu_A(x) : \Omega \rightarrow I$ .  $\mu_A(x)$  is called the membership function of  $A$  with  $0 \leq \mu_A(x) \leq 1$  for all  $x$  in  $\Omega$ . A family of fuzzy sets  $\delta$  is called a fuzzy topology for  $\Omega$ , and the pair  $(\Omega, \delta)$  is a fuzzy topological space if  $\delta$  satisfies the following conditions (Chang 1968):

- (i) The empty set  $\phi$  and the whole set  $\Omega$  belong to  $\delta$ .
- (ii) If  $A$  and  $B$  belong to  $\delta$ , then  $A \cap B \in \delta$ .
- (iii) Let  $\{A_k : k \in J\} \subset \delta$ , where  $J$  is an index set, then  $\cup_{k \in J} A_k \in \delta$ .

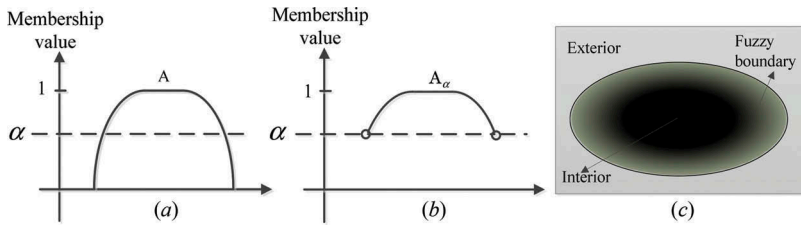


**Figure 2.** (a) Definition of fuzzy set  $A$  in real number, (b) interior of fuzzy set  $A$  ( $A_\alpha$ ), and (c) variation in density in a fuzzy set.

where  $\cap$  and  $\cup$  represent the intersection operation and union operation of the fuzzy sets, respectively.

Using fuzzy topology, a fuzzy set could be decomposed into three parts: interior, fuzzy boundary and exterior. According to Liu and Luo (1997), every interior operator corresponds to a fuzzy topology. Each interior operator can in turn be defined by a suitable level cut. Let  $\mu_A(x)$  be the membership function of a fuzzy set  $A$ , for a given positive value  $\alpha \in (0, 1)$ , we can define an interior operator (denoted as In-operator) as follows:

$$A_\alpha(x) = \begin{cases} A(x) & \text{if } \mu_A(x) > \alpha \\ 0 & \text{if } \mu_A(x) \leq \alpha, \end{cases} \quad (2)$$

as shown in Figure 2(b). The In-operator could induce a fuzzy topology, which is used to decompose the fuzzy sets (fuzzy classes) of DI in this work. As In-operator is a level cut operator, the fuzzy topology is called level cut fuzzy topology (LCFT).

### 2.2.2. Decompose DI with LCFT

The main idea of the second step of the proposed technique is to decompose DI with fuzzy topology. The membership functions of  $w_1$  and  $w_2$  classes have been computed in Section 2.1. In this part, we use the LCFT to decompose the two fuzzy classes of no-change and change, respectively. Each class is divided into three parts – interior, fuzzy boundary and exterior – by analysing its membership function.

According to the difference of the membership values of the pixels in  $P_{w_l}$  ( $l = 1, 2$ ), the fuzzy class  $w_l$  can be partitioned into the following three parts: interior  $w_l^o$ , fuzzy boundary  $\partial w_l$  and exterior  $X_D - w_l$ :

$$\begin{aligned} w_l^o &= (w_l)_{\alpha_l} = \{X_D(i, j) | P_{w_l}(X_D(i, j)) > \alpha_l\} \\ \partial w_l &= \{X_D(i, j) | 0.5 < P_{w_l}(X_D(i, j)) \leq \alpha_l\} \\ X_D - w_l &= \{X_D(i, j) | P_{w_l}(X_D(i, j)) \leq 0.5\} \end{aligned} \quad (3)$$

Here  $\alpha_l \in (0.5, 1)$  is a constant determined using the method provided in Section 2.2.3. Given that  $P_{w_1}(X_D(i, j)) + P_{w_2}(X_D(i, j)) = 1$  and considering the partition process, it is easy to show that  $X_D - w_1 = \partial w_2 \cup w_2^o$ ; that is the exterior of class  $w_1$  represents the interior and fuzzy boundary parts of  $w_2$ . In addition,  $X_D = w_1^o \cup \partial w_1 \cup (X_D - w_1)$ . Thus, the DI can be partitioned into three parts:

$$X_D = w_1^o \cup \partial w_1 \cup (\partial w_2 \cup w_2^o) = w_1^o \cup (\partial w_1 \cup \partial w_2) \cup w_2^o, \quad (4)$$

where  $w_1^o$ ,  $w_2^o$  and  $\partial w_1 \cup \partial w_2$  represent the interior of  $w_1$ , interior of  $w_2$  and fuzzy boundary region between  $w_1$  and  $w_2$ , respectively.

The dividing process demonstrates that the pixels having a low membership degree comprise the fuzzy boundary region  $\partial w_1 \cup \partial w_2$ . Therefore, the fuzzy boundary pixels are often misclassified and must be reclassified.

### 2.2.3. Determine the optimal threshold $\alpha_l$

The key to identifying the fuzzy boundary region of the DI is to determine the optimal threshold  $\alpha_l$  for  $w_l$ ,  $l = 1, 2$ . This study proposes an adaptive method to search the optimal threshold  $\alpha_l$  (ASOT). Since  $\alpha_l \in (0.5, 1)$ , it is reasonable to set the threshold search range as  $(0.5, 1)$ . Different searching paces can be applied to determine the optimal  $\alpha_l$  and we propose setting it as 0.05. Given a pixel  $X_D(i, j)$ , the higher the membership degree of  $w_l$ , the more likely it belongs to the interior of  $w_l$ . In this study, we suppose that the pixels with a membership degree larger than 0.99 will fall into the interior part. Accordingly, we select the optimal  $\alpha_l$  from the potential set

$$C = \{0.55, 0.60, 0.65, 0.70, 0.75, 0.80, 0.85, 0.90, 0.95, 0.99\}. \quad (5)$$

Ten parts of  $w_l$  can be obtained by Equation (5). The  $k$ th part  $(w_l)^k$  is defined as

$$(w_l)^k = \{X_D(i, j) | c_{k-1} < P_{w_l}(X_D(i, j)) < c_k\}, \quad (6)$$

where  $c_k$  is the  $k$ th element of the set  $C$  and  $c_0 = 0.5$ . Then, let  $N$  denotes the set  $\{n_k\}$ , where  $n_k$  denotes the number of pixels in  $(w_l)^k$ ,  $k = 1, 2, \dots, 10$ .

As each part  $(w_l)^k$  corresponds to equal range of membership grade (namely 0.05), the number of pixels in  $(w_l)^k$ , that is  $n_k$  could reflect the density of the part  $(w_l)^k$ . The interior part of fuzzy class  $w_l$  generally has a much greater density than the boundary part (Figure 2(c)). If the values increase sharply from  $n_k$  to  $n_{k+1}$ , then the densities significantly increase from  $(w_l)^k$  to  $(w_l)^{k+1}$ . Accordingly, we can expect that the parts  $(w_l)^k$  and  $(w_l)^{k+1}$  belong to the boundary and interior of  $w_l$ , respectively. We then assign  $c_k$  (the division of  $(w_l)^k$  and  $(w_l)^{k+1}$ ) to  $\alpha_l$ . That is, let  $\alpha_l = c_k$ .

As shown in Figure 3, in practice, if  $n_k, n_{k+1} > 0$  and  $n_{k+1} \geq 2 \times n_k$ , we think the values increase sharply from  $n_k$  to  $n_{k+1}$ . If there are more than one  $k$  meeting the above

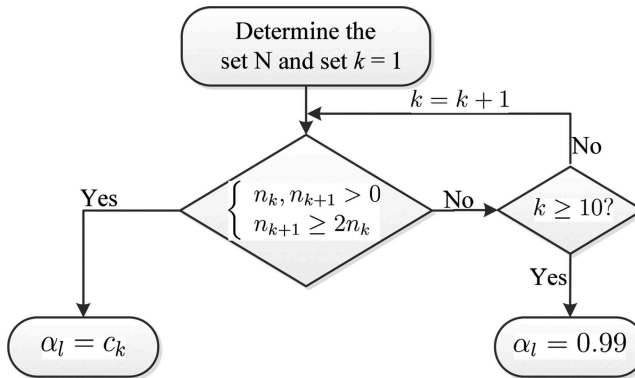


Figure 3. The searching process of the optimal  $\alpha_l$  for the fuzzy class  $w_l$ .

conditions, we assign the minimum  $c_k$  to  $a_l$ . If the  $k$  that satisfies the conditions above cannot be found, let  $a_l = 0.99$ .

### 2.3. Reclassify the fuzzy boundary pixels

Fuzzy topology can be used to describe and study the structure of a neighbourhood and the levelling of spaces (Liu, and Luo 1997). In Section 2.2, the fuzzy set  $w_l$  ( $l = 1, 2$ ) is divided by LCFT into interior and fuzzy boundary. The fuzzy topological relation of  $w_l$  is broken down by the In-operator in this process. The interior pixels are labelled as  $w_l$  and the boundary pixels must be reclassified. Since most of the spatial objects are spatial connected, the connectivity of spatial objects is important in spatial analysis. Also, the changes of spatial objects are more likely to occur in connected regions rather than at disjoint points.

This work uses the supported connectivity (Liu and Shi 2006) in the fuzzy topology to reclassify the pixels of fuzzy boundary, by which the fuzzy topology relation of class  $w_l$  ( $l = 1, 2$ ) are reconstructed. The details of this process are as follows: by searching the eight-neighbourhood of each boundary pixel  $X_D(i, j)$  and by recording each of its neighbour pixels, which belongs to the interior of a certain class ( $w_l$ ,  $l = 1$  or  $2$ ), this boundary pixel is reclassified as the class already assigned to the large number of neighbourhood pixels. If the number of pixels belonging to the interior of  $w_1$  is equal to that of  $w_2$  within its eight-neighbourhood, this boundary pixel is reclassified as class  $w_1$  if  $P_{w_1}(X_D(i, j)) \geq P_{w_2}(X_D(i, j))$ , and as class  $w_2$  otherwise. Note that if some of the boundary pixels are isolated from the interior pixels of both classes  $w_1$  and  $w_2$ , the process will be similar with the seeded region growing (Adams and Bischof 1994).

## 3. Experimental results

Two experimental studies were conducted to assess the performance of the proposed FTCD framework. Quantitative analysis of the change detection results were carried out in terms of: (1) missed detection (MD), (2) false alarm (FA), (3) total error (TE), (4) Kappa coefficient ( $\kappa$ ) and (5) measure of quality (QM) (Rutzinger, Rottensteiner, and Pfeifer 2009; Bovolo, Bruzzone, and Marconcini 2008). The experiments were conducted with MATLAB 2012 on a computer that has Intel(R) Core(TM) i5-2400 3.1 GHz processor and 4 GB RAM. Time consumption was recorded to compare the time complexity of different methods.

### 3.1. Dataset description

Two different real datasets were adopted in the experimental study. The first dataset is a section ( $400 \times 400$  pixels) of two Landsat 7 ETM+ images acquired in August 2001 and August 2002 in Liaoning province, China. The 2001 image was radiometrically corrected through histogram matching method to the 2002 image. The second dataset, available from the homepages (<http://see.xidian.edu.cn/faculty/mggong/Projects/iCD.htm>), is a section ( $412 \times 300$  pixels) of two Landsat 5 TM images acquired in September 1995 and July 1996 on the Island of Sardinia, Italy. The histogram matching approach was applied to the September image by referencing the July image for the relative radiometric correction. In addition, the dataset used in each experiment is acquired in the same season. Thus, it is reasonable that phenological changes are negligible. Figure 4

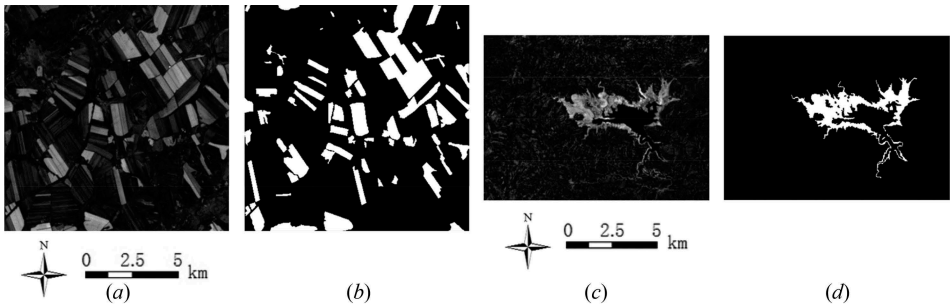


**Figure 4.** Difference images of (a) Liaoning data (the centre coordinate: 48°3'N, 126°8'E) and (c) Sardinia data (the centre coordinate: 39°37'N, 9°13'E); and the ground reference maps of (b) Liaoning data and (d) Sardinia data.

shows the corresponding DIs and the ground reference maps of change. The ground reference map is manually generated according to a detailed visual analysis of both the available multitemporal images and the DI.

3.2. Experimental results and discussion

To evaluate the effectiveness of the proposed FTCD framework, six change detection methods were compared, namely Kittler (Patra, Ghosh, and Ghosh 2011), ACM (Bazi *et al.* 2010), EM, Kapur, FT-EM and FT-Kapur. Tables 1 and 2 show the quantitative change detection results for the Liaoning data and the Sardinia data, respectively. Figures 5 and 6 depict the change detection maps and the partitioned results of the DIs. In the partitioned results, black denotes the interior of  $w_1$ , white the interior of  $w_2$  and red the fuzzy boundary region between  $w_1$  and  $w_2$ .

Tables 1 and 2 show that the proposed FTCD approaches (FT-EM and FT-Kapur) produce better change detection results than the corresponding standard methods (EM and Kapur) in terms of total error, measure of quality and Kappa coefficient. As an example, on Liaoning data, for FT-EM compared with EM, the total error decreases from 11,032 to 8071, measure of quality increases from 0.7203 to 0.7752 and Kappa values increase from 0.7943 to 0.8420. Experimental results indicate that the fuzzy

**Table 1.** Quantitative change detection results for the Liaoning data.

Methods used	MD (n)	FA (n)	TE (n)	QM (%)	$\kappa$	Time (s)
Kittler	2125	7815	9940	0.7392	0.8112	2.4
ACM	7604	4151	11755	0.6588	0.7835	6.3
EM	1886	9146	11032	0.7203	0.7943	3.94
FT-EM	2467	5604	8071	0.7752	0.8420	4.50
Kapur	3050	4108	7158	0.7919	0.8527	0.41
FT-Kapur	3751	2637	6388	0.8060	0.8681	0.78

**Table 2.** Quantitative change detection results for the Sardinia data.

Methods used	MD (n)	FA (n)	TE (n)	QM (%)	$\kappa$	Time (s)
Kittler	77	12747	12824	0.3705	0.4976	2.1
ACM	929	1767	2696	0.7130	0.8208	5.2
EM	385	8528	8913	0.4482	0.5844	3.03
FT-EM	420	5830	6250	0.5355	0.6719	3.32
Kapur	839	2233	3072	0.6884	0.8022	0.39
FT-Kapur	810	1810	2620	0.7223	0.8275	0.67



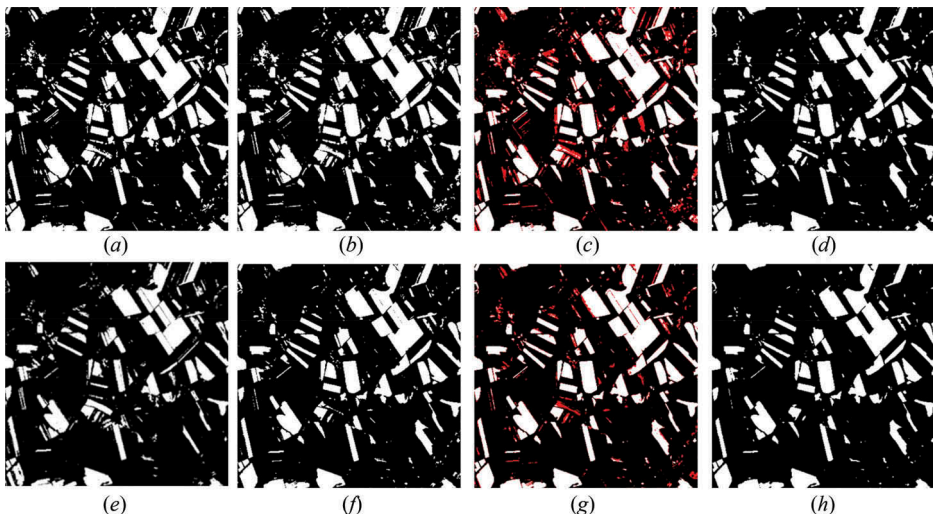


**Figure 5.** Change detection maps obtained for Liaoning data using (a) Kittler, (b) EM, (d) FT-EM, (e) ACM, (f) Kapur and (h) FT-Kapur; and the partitioned results used in (c) FT-EM and (g) FT-Kapur for Liaoning DI (black is the interior of  $w_1$ , white the interior of  $w_2$  and red the fuzzy boundary region between  $w_1$  and  $w_2$ ).

topology-based methods perform better than traditional thresholding techniques. This is because the algorithms based on fuzzy topology can identify the fuzzy boundary pixels that have a low membership grade; these pixels are then effectively reclassified using the supported connectivity. The identified boundary pixels of each experiment (marked as red in Figures 5 and 6) correspond to the patterns having more uncertainty than other pixels. Thus, the effective reclassification process leads to an improvement on the change detection results.

To evaluate the effect of the reclassifying process, the performances of the FTCD method and standard method on the fuzzy boundary pixels were compared. Table 3 lists the change detection results of the determined fuzzy boundary pixels, where FBN and FBA are the number of the fuzzy boundary pixels and change detection accuracy, respectively. As reported in Table 3, for both the experiments executed, the FT-EM and FT-Kapur achieve comparatively higher change detection accuracies than the standard methods (i.e. EM and Kapur) in terms of the identified fuzzy boundary pixels. For example, for the Liaoning dataset, 9944 boundary pixels were identified in the FT-EM, and the accuracy of the determined boundary pixels of FT-EM is about 76.5%, which represents an improvement about 30% from that of EM.

Tables 1 and 2 also show that FT-Kapur achieves better results than FT-EM. This is because Kapur produces better change detection results than EM. However, FT-EM produces a comparatively higher improvement on both Kappa coefficient and total error than the FT-Kapur in comparison with the results of the corresponding standard method for the same remotely sensed image, respectively. The reason for this is that the change map yielded by EM contains much more white noise spots compared with that of Kapur (Figures 5 and 6), and has more fuzzy boundary (uncertain) pixels to be further processed (Table 3). Dealing with more uncertain pixels leads to the FT-EM gaining higher improvement than FT-Kapur compared with the corresponding standard method.

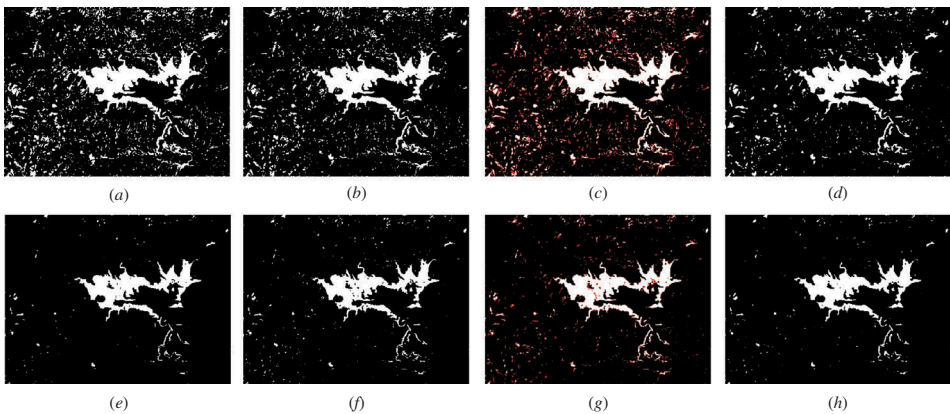


**Figure 6.** Change detection maps obtained for the Sardinia data using (a) Kittler, (b) EM, (d) FT-EM, (e) ACM, (f) Kapur and (h) FT-Kapur; and the partitioned results used in (c) FT-EM and (g) FT-Kapur for Sardinia DI (black is the interior of  $w_1$ , white the interior of  $w_2$  and red the fuzzy boundary region between  $w_1$  and  $w_2$ ).

**Table 3.** Change detection results on the fuzzy boundary pixels.

Methods used	Liaoning data		Sardinia data	
	FBN	FBA (%)	FBN	FBA (%)
EM	9944	46.72	7779	53.95
FT-EM		76.53		88.27
Kapur		56.74		70.61
FT-Kapur		72.85		84.56

For the Liaoning dataset, both the proposed FTCD methods FT-EM and FT-Kapur perform better than Kittler and ACM. For Sardinia dataset, FT-Kapur produces the best change detection results. However, the change detection accuracy of FT-EM is lower than that of ACM, which is due to the bad change detection results of EM.

With regard to the computation time complexity, the proposed FTCD approach has slightly higher computation time requirement than the corresponding standard one, but Kapur and FT-Kapur are much faster than other methods. Experimental results indicate that the proposed FTCD framework can address the problem of uncertain region of the standard thresholding method (e.g. EM and Kapur) at a low cost of time complexity.

4. Conclusions

This study proposed a fuzzy topology-based framework for the analysis of the DI in unsupervised change detection problems. In the framework, the DI is first classified into two categories: unchanged ( $w_1$ ) and changed ( $w_2$ ). It is then partitioned into three parts – interior of  $w_1$ , interior of  $w_2$  and fuzzy boundary region between  $w_1$  and  $w_2$  – using fuzzy topology. Finally, the fuzzy boundary pixels (having more uncertainty) are reclassified based on the supported connectivity of fuzzy topology to enhance the performance of change detection. In the theoretical aspect, the fuzzy topology is first introduced into change detection problem, which contributes to the development of the technique of analysing DI. In the methodological aspect, a novel change detection

framework based on fuzzy topology is proposed; two threshold methods belonging to the FTCD framework have been investigated. Two different experiments were carried out and the results confirm the effectiveness of the given technique.

## Acknowledgements

The authors thank Prof. Gong for providing the Sardinia dataset and the editors and anonymous reviewers for their insightful comments and valuable suggestions.

## Disclosure statement

No potential conflict of interest was reported by the authors.

## Funding

This work was supported by the Ministry of Science and Technology of China [project number 2012BAJ15B04].

## References

- Adams, R., and L. Bischof. 1994. "Seeded Region Growing." *IEEE Transactions on Pattern Analysis and Machine Intelligence* 16: 641–647. doi:[10.1109/34.295913](https://doi.org/10.1109/34.295913).
- Bazi, Y., F. Melgani, and H. D. Al-Sharari. 2010. "Unsupervised Change Detection in Multispectral Remotely Sensed Imagery with Level Set Methods." *IEEE Transactions on Geoscience and Remote Sensing* 48: 3178–3187. doi:[10.1109/TGRS.2010.2045506](https://doi.org/10.1109/TGRS.2010.2045506).
- Bovolo, F., L. Bruzzone, and M. Marconcini. 2008. "A Novel Approach to Unsupervised Change Detection Based on a Semisupervised SVM and a Similarity Measure." *IEEE Transactions on Geoscience and Remote Sensing* 46: 2070–2082. doi:[10.1109/TGRS.2008.916643](https://doi.org/10.1109/TGRS.2008.916643).
- Bruzzone, L., and F. Bovolo. 2013. "A Novel Framework for the Design of Change-Detection Systems for Very-High-Resolution Remote Sensing Images." *Proceedings of the IEEE* 101: 609–630. doi:[10.1109/JPROC.2012.2197169](https://doi.org/10.1109/JPROC.2012.2197169).
- Bruzzone, L., and D. F. Prieto. 2000. "Automatic Analysis of the Difference Image for Unsupervised Change Detection." *IEEE Transactions on Geoscience and Remote Sensing* 38: 1171–1182. doi:[10.1109/36.843009](https://doi.org/10.1109/36.843009).
- Celik, T., and K.-K. Ma. 2010. "Unsupervised Change Detection for Satellite Images Using Dual-Tree Complex Wavelet Transform." *IEEE Transactions on Geoscience and Remote Sensing* 48: 1199–1210. doi:[10.1109/TGRS.2009.2029095](https://doi.org/10.1109/TGRS.2009.2029095).
- Chang, C. L. 1968. "Fuzzy Topological Spaces." *Journal of Mathematical Analysis and Applications* 24: 182–190. doi:[10.1016/0022-247X\(68\)90057-7](https://doi.org/10.1016/0022-247X(68)90057-7).
- Ghosh, A., N. S. Mishra, and S. Ghosh. 2011. "Fuzzy Clustering Algorithms for Unsupervised Change Detection in Remote Sensing Images." *Information Sciences* 181: 699–715. doi:[10.1016/j.ins.2010.10.016](https://doi.org/10.1016/j.ins.2010.10.016).
- Liu, K., and W. Shi. 2006. "Computing the Fuzzy Topological Relations of Spatial Objects Based on Induced Fuzzy Topology." *International Journal of Geographical Information Science* 20: 857–883. doi:[10.1080/13658810600711345](https://doi.org/10.1080/13658810600711345).
- Liu, Y. M., and M. K. Luo. 1997. *Fuzzy Topology*. Singapore: World Scientific.
- Patra, S., S. Ghosh, and A. Ghosh. 2011. "Histogram Thresholding for Unsupervised Change Detection of Remote Sensing Images." *International Journal of Remote Sensing* 32: 6071–6089. doi:[10.1080/01431161.2010.507793](https://doi.org/10.1080/01431161.2010.507793).
- Rutzinger, M., F. Rottensteiner, and N. Pfeifer. 2009. "A Comparison of Evaluation Techniques for Building Extraction from Airborne Laser Scanning." *IEEE Journal of Selected Topics in Applied Earth Observations and Remote Sensing* 2: 11–20. doi:[10.1109/JSTARS.2009.2012488](https://doi.org/10.1109/JSTARS.2009.2012488).